

Relationship Between the Magnetic Flux of Solar Eruptions and the A_p Index of Geomagnetic Storms

I.M. Chertok · M.A. Abunina · A.A. Abunin ·
A.V. Belov · V.V. Grechnev

Received: 26 June 2014 / Accepted: 23 October 2014 / Published online: 4 November 2014
© Springer Science+Business Media Dordrecht 2014

Abstract Solar coronal mass ejections (CMEs) are the main drivers of the most powerful non-recurrent geomagnetic storms. In the extreme-ultraviolet range, CMEs are accompanied by bright post-eruption arcades and dark dimmings. The analysis of events of Solar Cycle 23 (Chertok *et al.* in *Solar Phys.* **282**, 175, 2013) revealed that the summarized unsigned magnetic flux in the arcades and dimming regions at the photospheric level, Φ , is significantly related to the intensity (Dst index) of geomagnetic storms. This provides the basis for the earliest diagnostics of geoefficiency of solar eruptions. In the present article, using the same data set, we find that a noticeable correlation also exists between the eruptive magnetic flux, Φ , and another geomagnetic index, A_p . As the magnetic flux increases from some tens to ≈ 500 (in units of 10^{20} Mx), the geomagnetic storm intensity measured by the three-hour A_p index increases on average from $A_p \approx 50$ to a formal upper limit of 400 (in units of 2 nT). The established relationship shows that the real value of the A_p index is not limited and during the most severe magnetic storms may significantly exceed 400.

Keywords Solar eruptions · Arcades · Coronal dimming · Coronal mass ejections · Magnetic fields · Geomagnetic storms

1. Introduction

Intense non-recurrent geomagnetic storms (GMSs) are the most significant space weather disturbances. In contrast to relatively weak recurrent storms associated with high-speed solar wind streams from coronal holes, they are initiated by coronal mass ejections (CMEs) and their interplanetary extensions (ICMEs) (*e.g.*, Bothmer and Zhukov, 2007; Gopalswamy,

I.M. Chertok (✉) · M.A. Abunina · A.A. Abunin · A.V. Belov
Pushkov Institute of Terrestrial Magnetism, Ionosphere and Radio Wave Propagation (IZMIRAN),
Troitsk, Moscow Region, 142190, Russia
e-mail: ichertok@izmiran.ru

V.V. Grechnev
Institute of Solar-Terrestrial Physics SB RAS, Lermontov St. 126A, Irkutsk 664033, Russia
e-mail: grechnev@iszf.irk.ru

2009). A GMS occurs when a large and fast CME/ICME transports to Earth a magnetic field with a sufficiently strong and prolonged southward (negative) B_z component. One of the most important tasks of the solar-terrestrial physics and space weather prediction is diagnostics of the geoeffectiveness of CMEs, *i.e.*, a quantitative forecast of a possible non-recurrent GMS from observed characteristics of the eruption that just occurred. Existing algorithms of this diagnostics are based in one way or another on the measurements of the CME speed and shape in the plane of the sky near the Sun (Gopalswamy, 2009; Kim *et al.*, 2010).

We develop another approach to the early diagnostics of solar eruptions, in which quantitative characteristics of such large-scale CME manifestations as post-eruption (PE) arcades and dimmings observed in the extreme ultraviolet (EUV) range are used as key parameters instead of the projected CME speed and shape (Chertok and Grechnev, 2006; Chertok *et al.*, 2013). Dimmings are CME-associated regions in which the EUV (and soft X-ray) brightness of coronal structures is temporarily reduced during an ejection and persists over many hours (Thompson *et al.*, 1998; Webb *et al.*, 2000; Hudson and Cliver, 2001). The deepest stationary long-lived dimmings adjacent to the eruption center are interpreted mainly as a result of plasma outflow and density decrease in footpoints of erupting and expanding CME flux ropes. Large-scale arcades of bright loops enlarging in size over time arise at the place of the main body of pre-eruption magnetic flux ropes ejected as CMEs (Kahler, 1977; Sterling *et al.*, 2000; Tripathi, Bothmer, and Cremades, 2004). As a whole, PE arcades and dimmings visualize the structures and areas involved in the processes of CME eruptions.

A number of studies indicate that parameters of CMEs and near-Earth magnetic clouds (MCs) are governed by total magnetic fluxes in their solar source regions. Qiu and Yurchyshyn (2005) found a correlation between the CME speed and the total reconnected flux in associated flares. Leamon *et al.* (2004) and Mandrini *et al.* (2005) demonstrated that the total magnetic fluxes in MCs estimated from *in situ* measurements near Earth and their solar sources were close to each other. Webb *et al.* (2000) and Attrill *et al.* (2006) found a similarity between the magnetic fluxes in MCs and dimming regions. Qiu *et al.* (2007) and Hu *et al.* (2014) found this similarity for the reconnected magnetic flux in several events. Therefore, a correspondence is expected between the magnetic flux involved in an eruption on the one hand and the parameters of the associated geospace disturbances on the other hand. If a magnetic cloud carries a negative B_z component, then a correlation might be expected between the magnetic fluxes in eruption regions and the intensities of the GMSs that they produce.

Chertok *et al.* (2013) established that a statistical dependence of the GMS intensity measured by the Dst index (as well as of the onset and peak GMS transit times and Forbush decrease magnitudes) on the eruptive magnetic flux in the arcades and dimming regions, Φ , does exist. The aim of the present work is to analyze the relationship between this eruptive flux Φ and another geomagnetic index A_p that also characterizes the GMS intensity and is often used in solar-terrestrial forecasting.

2. Analyzed Parameters and Data

We recall that the hourly storm-time disturbance index Dst (see <http://wdc.kugi.kyoto-u.ac.jp/dstdir/index.html>) is calculated from data of four low-latitude geomagnetic observatories and characterizes the effect of the global equatorial ring current. The latter is manifested in the inner magnetosphere and causes a decrease of the horizontal component of the terrestrial magnetic field during the main phase of GMSs. The linear planetary three-hour A_p index,

considered below, characterizes the strength of auroral currents. The Ap index is defined as the mean value of the variations of the terrestrial magnetic field, which corresponds to a logarithmic Kp index, measured by data of 13 geomagnetic stations located at moderately high geomagnetic latitudes mainly in the northern hemisphere (Siebert and Meyer, 1996; Zabolotnaya, 2007). The Ap index varies from 0 to a formally highest value of 400 corresponding to Kp = 9, and is measured in units of 2 nT (hereinafter, as is often done, we will omit the units). We emphasize that the formal upper limit of Ap = 400 is a condition that appears as a result of the conversion of Ap from Kp indices. In a physical sense, the Ap index is not limited. It is determined by real variations of the terrestrial magnetic field components and during the strongest magnetic storms can considerably exceed 400. Features of the Dst and Ap indices are such that relationships between them in concrete events may be different, depending on the impact of an ICME on the equatorial and auroral current systems. In addition, the peak time of the Dst and Ap indices are not always identical and may differ by a few hours.

We consider the same ensemble of events that has been analyzed by Chertok *et al.* (2013): strong non-recurrent GMSs during Solar Cycle 23 (1996–2008) with $Dst \leq -100$ nT, which reliably or with a high probability are identified with a concrete eruption from the central zone of the visible solar hemisphere within $\pm 45^\circ$ from the central meridian. We distinguish events caused by eruptions that occurred in active regions (ARs), and events associated with filament eruptions outside ARs referring to them as AR events and non-AR events. These two categories of events differ significantly in the characteristics of accompanying arcades and dimmings, properties of CMEs/ICMEs, and intensity of GMSs that they cause (e.g., Švestka, 2001).

Our source data are the EUV solar images obtained with the *Extreme ultraviolet Imaging Telescope* (EIT: Delaboudinière *et al.*, 1995) in the 195 Å channel and the magnetograms obtained with the *Michelson Doppler Imager* (MDI: Scherrer *et al.*, 1995), both onboard the *Solar and Heliospheric Observatory* (SOHO: Domingo, Fleck, and Poland, 1995). For each of the analyzed events, after a routine processing of the corresponding FITS files, the solar rotation in the analyzed images was compensated, and then the same fixed image before an eruption was subtracted from all subsequent images to obtain fixed-base difference images (Chertok and Grechnev, 2005). Significant regions of the arcades and dimmings were extracted following selected relative (not absolute) criteria of brightness variations. The analysis showed that a brightness depression of more than 40 % from the pre-eruption level was the best criterion for extracting relevant significant dimmings. For PE arcades, an appropriate criterion was to extract the area around the eruption center where the brightness in the 195 Å channel exceeded 5 % of the highest brightness. A total (unsigned) eruptive magnetic flux within the extracted arcade and dimming areas was evaluated at the photospheric level by co-aligning the resulting EIT difference images with an MDI line-of-sight magnetogram recorded just before an eruption. A detailed description of all required procedures is given in Chertok *et al.* (2013).

Here we characterize the highest intensity of GMSs by a peak in the three-hour Ap index, the values of which are determined in the GeoForschungsZentrum (GFZ), Potsdam, and presented at <http://ftp.gfz-potsdam.de/pub/home/obs/kp-ap/wdc/>. The comprehensive list of the analyzed events and their parameters are shown in a table displayed at the site <http://www.izmiran.ru/~ichertok/Ap/>. The table includes 90 events and contains in particular the following data: the numbers of the GMS events according to the Coordinated Data Analysis Workshop (CDAW) catalog (Zhang *et al.*, 2007); information on date, time, and intensity of a GMS, including Ap index; data about the eruption, which reliably or with a high probability was a source of the given GMS; the total magnetic fluxes in the arcades and dimming regions; and some others.

3. Results

First, we consider the events in which a GMS is reliably identified with a particular solar eruption. Figure 1a shows the location of such events on the plot of “the geomagnetic A_p index vs. the eruptive magnetic flux in the arcades and dimming regions, Φ ”. In this figure and the following ones, the diamonds denote the AR eruptions, the triangles correspond to the non-AR eruptions.

As noted by Chertok *et al.* (2013), a few events associated with filament eruptions outside ARs (non-AR events) form a separate group, which is markedly different from the events produced by the eruptions in ARs (AR events). The non-AR events are characterized by relatively low magnetic fluxes, $\Phi < 80 \times 10^{20}$ Mx, but they can cause GMSs with $A_p > 200$. Figure 1 does not show any pronounced dependence of A_p on Φ for such events. A possible reason for these features of the non-AR events is that the criteria for extracting significant arcades and dimmings accepted for the AR events are not entirely suitable for the non-AR events. It is known (Švestka, 2001) that filament eruptions outside ARs are accompanied by relatively weak but more extensive PE arcades as well as by shallower dimmings than are seen in eruptions in ARs. This suggests that the relative thresholds of the brightness variations for the extraction of the arcades and dimmings indicated above should be optimized at lower levels for the non-AR events. In this case, the values of the eruptive magnetic flux would noticeably increase, but in different ways for different events. Some other factors may also affect the characteristics of GMSs caused by the non-AR eruptions. Therefore, the non-AR events require a special additional analysis and were not included in the remainder of this article.

Among the AR events (diamonds), attention should be paid to an event that strongly deviates from other GMSs. This is the famous exceptional event of 18–20 November 2013, in which under relatively small eruptive magnetic flux $\Phi \approx 133 \times 10^{20}$ Mx the GMS intensity reached $A_p \approx 300$ (this storm was the strongest in Solar Cycle 23 in terms of the index $Dst \approx -422$ nT). The causes of the exceptional properties of this extreme event are analyzed in detail by Grechnev *et al.* (2014). The authors showed in particular that the GMS

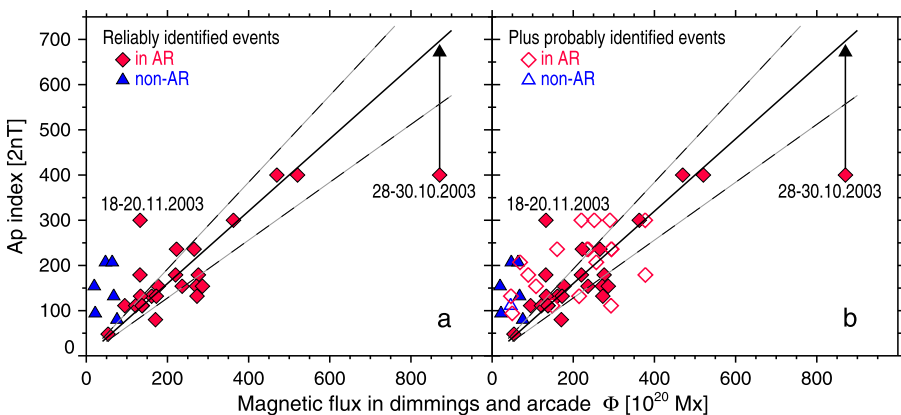


Figure 1 Dependence of the geomagnetic A_p index on the total magnetic flux in the arcades and dimming regions Φ : (a) for GMSs reliably identified with a definite solar eruption (filled symbols) and (b) for all considered events including those with probable solar source identification (open symbols). Red diamonds denote eruptions in ARs, blue triangles denote eruptions of filaments outside ARs. The dashed lines delimit the adopted 20 % deviation band.

was caused by arrival to Earth of a compact spheromak with a magnetic field strength of up to $|B| \approx 56$ nT and a large, prolonged southern component $B_z \approx -46$ nT. Such a strong field strong in the interplanetary magnetic cloud was preserved due to its anomalously weak expansion in the propagation from the Sun to Earth. Below we do not consider this event because of its atypical properties.

The remaining reliably identified AR events, shown in Figure 1a, demonstrate a significant relation between the eruptive flux Φ and the geomagnetic index A_p . When the flux Φ increases from some tens to about 500 (in 10^{20} Mx units), the A_p index increases to the formally highest value of 400. Three events with the strongest eruptive flux indicate this dependence at the formal peak level $A_p = 400$. Real values of the A_p index for these three events are not given in catalogs. We temporarily discard the 28–30 October 2003 event with the strongest magnetic flux Φ and assume that for two events with the magnetic flux Φ in a range of $(470–520) \times 10^{20}$ Mx the formal index $A_p = 400$ was close to the real one. Then the dependence of the A_p index on the eruptive magnetic flux Φ for the AR events can be expressed by a linear relation $A_p = 0.8\Phi$ (here again Φ is expressed in units of 10^{20} Mx). In this case, the correlation coefficient between the observed and calculated values of A_p reaches $r \approx 0.90$. For an additional evaluation of the scatter in data points, we chose a deviation band bounded by ± 0.2 from the regression line that appears to be acceptable for the forecasting. Calculations show that 14 out of 22 events (*i.e.*, 64 %) fall into this deviation band.

Extrapolation the obtained relation allows us to estimate a probable increase of the real A_p index for eruptions with the strongest magnetic flux without the formal upper limit of $A_p = 400$. In particular, for the 28–30 October 2003 event with $\Phi \approx 870 \times 10^{20}$ Mx, the A_p index, in accordance with this dependence, should be around 700. This estimate does not contradict the largest variations of the horizontal component of the Earth's magnetic field (about 1700–2500 nT) registered by high-latitude magnetometers (*e.g.*, Panasyuk *et al.*, 2004). According to the data of the magnetic observatory Moscow (IZMIRAN), in the period 21–24 UT on 29 October 2003 the field variations were about 1200 nT, that yields $A_p \approx 800$. This also agrees well with the dependence presented above.

The dependence of the geomagnetic A_p index on the eruptive magnetic flux Φ for the AR events appears to be basically the same when the GMSs with a probable source identification (open symbols in Figure 1b) are added to the unambiguously identified events. Here, as expected, the scatter of the points increases, and the correlation coefficient between Φ and A_p reduces to $r \approx 0.73$. In this case, 19 points out of 41 (*i.e.*, 46 %) fall into the same deviation band.

4. Conclusions

Our analysis has shown that for AR events a noticeable statistical relationship exists between the GMS intensity measured by the A_p index and the eruptive magnetic flux Φ in solar EUV arcades and dimming regions. This relationship also demonstrates that solar eruptions with the greatest magnetic flux can lead to the strongest GMSs, in which a real A_p index significantly exceeds the formally introduced highest level of $A_p = 400$.

This result is consistent with those reported by Chertok *et al.* (2013), who established the dependencies on the same eruptive magnetic flux, Φ , for important space weather parameters such as i) the intensity of GMSs characterized by another geomagnetic index Dst, ii) the values of the Forbush decreases (FDs) of the galactic cosmic-ray flux, and iii) the onset and peak times of these disturbances. This means that although many factors affect

the propagation of interplanetary clouds from the Sun to Earth and the character of their interaction with the Earth's magnetosphere, the parameters of non-recurrent GMSs (and FDs) caused by CMEs/ICMEs are largely determined by the power of solar eruptions (in terms of the total magnetic flux in dimmings and arcades). This is especially conspicuous for large eruptions. Just because of this, statistical relationships exist between the magnetic flux in the source region of a CME on the one hand and the main parameters of GMSs and FDs on the other hand.

The positive results of the present work and the analysis of Chertok *et al.* (2013) demonstrate the relevance of the magnetic flux in arcades and dimmings as a diagnostic parameter. This parameter can be used for the earliest estimations of the intensity and temporal characteristics of GMSs (and FDs), including both Dst and Ap indices, even without taking into account the information on associated CMEs and factors determining the B_z component. At present, we considered only intense GMSs. Therefore, when the GMS amplitude is estimated on the basis of the dependencies established in this article and by Chertok *et al.* (2013), it refers to a value close to the maximum that can be expected when an ICME contains a significant negative (southern) B_z component. The proposed tool for the early diagnostics of the geoeffectiveness of a solar eruption should be considered and used as an initial component of a wider complex of methods of the short-term GMS and FD forecasting, also including those based on the measurements of near-the-Sun CMEs, MHD models, stereoscopic observations of ICME propagation, and others.

Acknowledgements We are grateful to an anonymous referee for constructive comments that helped us to improve the manuscript. The authors thank the SOHO EIT and MDI teams as well as the CDAW participants for data and materials used in the present study. SOHO is a project of international cooperation between ESA and NASA. This research was supported by the Russian Foundation of Basic Research under grants 12-02-00037, 14-02-00367, and the Ministry of education and science of Russian Federation under projects 8407 and 14.518.11.7047.

References

- Attrill, G., Nakwacki, M.S., Harra, L.K., van Driel-Gesztelyi, L., Mandrini, C.H., Dasso, S., Wang, J.: 2006, *Solar Phys.* **238**, 117. DOI.
- Bothmer, V., Zhukov, A.: 2007, In: Bothmer, V., Daglis, I.A. (eds.) *Space Weather – Physics and Effects*, 31.
- Chertok, I.M., Grechnev, V.V.: 2005, *Solar Phys.* **229**, 95. DOI.
- Chertok, I.M., Grechnev, V.V.: 2006, *Bull. Russ. Acad. Sci., Phys.* **70**, 1717.
- Chertok, I.M., Grechnev, V.V., Belov, A.V., Abunin, A.A.: 2013, *Solar Phys.* **282**, 175. DOI.
- Delaboudinière, J.-P., Artzner, G.E., Brunaud, J., Gabriel, A.H., Hochedez, J.F., Millier, F., *et al.*: 1995, *Solar Phys.* **162**, 291. DOI.
- Domingo, V., Fleck, B., Poland, A.I.: 1995, *Solar Phys.* **162**, 1. DOI.
- Gopalswamy, N.: 2009, In: Tsuda, T., Fujii, R., Shibata, K., Geller, M.A. (eds.) *Climat and Weather of the Sun–Earth Syst. (CAWSES): Selected Papers from the 2007 Kyoto Symp.*, 77.
- Grechnev, V.V., Uralov, A.M., Chertok, I.M., Belov, A.V., Filippov, B.P., Slemzin, V.A., Jackson, B.V.: 2014, *Solar Phys.*, in press. DOI.
- Hu, Q., Qiu, J., Dasgupta, B., Khare, A., Webb, G.M.: 2014, *Astrophys. J.* **793**, article id. 53. DOI.
- Hudson, H.S., Cliver, E.W.: 2001, *J. Geophys. Res.* **106**, 25199. DOI.
- Kahler, S.: 1977, *Astrophys. J.* **214**, 891. DOI.
- Kim, R.-S., Cho, K.-S., Moon, Y.-J., Dryer, M., Lee, J., Yi, Y., *et al.*: 2010, *J. Geophys. Res.* **115**, A12108. DOI.
- Leamon, R.J., Canfield, R.C., Jones, S.L., Lambkin, K., Lundberg, B.J., Pevtsov, A.A.: 2004, *J. Geophys. Res.* **109**, 5106. DOI.
- Mandrini, C.H., Pohjolainen, S., Dasso, S., Green, L.M., Démoulin, P., van Driel-Gesztelyi, L., Copperwheat, C., Foley, C.: 2005, *Astron. Astrophys.* **434**, 725. DOI.
- Panasyuk, M.I., Kuznetsov, S.N., Lazutin, L.L., Avdyushin, S.I., Alexeev, I.I., Ammosov, P.P., *et al.*: 2004, *Cosm. Res.* **42**, 489. DOI.

- Qiu, J., Yurchyshyn, V.B.: 2005, *Astrophys. J. Lett.* **634**, L121. DOI.
- Qiu, J., Hu, Q., Howard, T.A., Yurchyshyn, V.B.: 2007, *Astrophys. J.* **659**, 758. DOI.
- Scherrer, P.H., Bogart, R.S., Bush, R.I., Hoeksema, J.T., Kosovichev, A.G., Schou, J., *et al.*: 1995, *Solar Phys.* **162**, 129. DOI.
- Siebert, M., Meyer, J.: 1996, In: Dieminger, W., Hartmann, G.K., Leitinger, R. (eds.) *The Upper Atmosphere*, 887.
- Sterling, A.C., Hudson, H.S., Thompson, B.J., Zarro, D.: 2000, *Astrophys. J.* **532**, 628. DOI.
- Švestka, Z.: 2001, *Space Sci. Rev.* **95**, 135.
- Thompson, B.J., Plunkett, S.P., Gurman, J.B., Newmark, J.S., St. Cyr, O.C., Michels, D.J.: 1998, *Geophys. Res. Lett.* **25**, 2465. DOI.
- Tripathi, D., Bothmer, V., Cremades, H.: 2004, *Astron. Astrophys.* **422**, 337. DOI.
- Webb, D.F., Lepping, R.P., Burlaga, L.F., DeForest, C.E., Larson, D.E., Martin, S.F., *et al.*: 2000, *J. Geophys. Res.* **105**, 27251. DOI.
- Zabolotnaya, N.A.: 2007, *Indices of Geomagnetic Activity*, LKI, Moscow. (In Russian).
- Zhang, J., Richardson, I.G., Webb, D.F., Gopalswamy, N., Huttunen, E., Kasper, J., *et al.*: 2007, *J. Geophys. Res.* **112**, A10102. DOI.